IOPscience iopscience.iop.org

Home Search Collections Journals About Contact us My IOPscience

On the size of sports fields

This content has been downloaded from IOPscience. Please scroll down to see the full text.

2014 New J. Phys. 16 033039

(http://iopscience.iop.org/1367-2630/16/3/033039)

View the table of contents for this issue, or go to the journal homepage for more

Download details:

IP Address: 130.126.255.92
This content was downloaded on 03/12/2015 at 17:19

Please note that terms and conditions apply.

New Journal of Physics
The open access journal at the forefront of physics
Deutsche Physikalische Gesellschaft DPG | IOP Institute of Physics

On the size of sports fields

Baptiste Darbois Texier[1], Caroline Cohen[1], Guillaume Dupeux[2], David Quéré[2] and Christophe Clanet[1]

[1] LADHYX, UMR 7646 du CNRS, École Polytechnique, 91128 Palaiseau Cedex, France
[2] PMMH, UMR 7636 du CNRS, ESPCI, 75005 Paris, France
E-mail: clanet@ladhyx.polytechnique.fr

Received 8 September 2013
Accepted for publication 4 February 2014
Published 28 March 2014

New Journal of Physics **16** (2014) 033039

doi:10.1088/1367-2630/16/3/033039

Abstract

The size of sports fields considerably varies from a few meters for table tennis to hundreds of meters for golf. We first show that this size is mainly fixed by the range of the projectile, that is, by the aerodynamic properties of the ball (mass, surface, drag coefficient) and its maximal velocity in the game. This allows us to propose general classifications for sports played with a ball.

Keywords: physics of sports, aerodynamics, ballistics, ball trajectory, ball sports

One could think that the size of a sports field is a function of the number of players, of the rules, of the ball shape, or of the way of launching the ball [1]. We focus here on the role of the ball range, that is, the maximal distance that the ball can travel in one shot. Due to its application in the military context [2], and more recently in sports [3], this ballistic problem has been studied in detail for a long time, and geometrical constructions [4], numerical solutions [5] and theoretical discussions [6, 7] have been proposed for approaching the actual trajectory.

One famous early work on the subject is 'Dialogues Concerning Two New Sciences' [8] published in 1638 by Galileo, one century after 'triangular trajectories' were reported by Tartaglia [9, 10]. Here, we revisit the problem with a special focus on the maximal range and then study its correlation with the size of sports fields.

Content from this work may be used under the terms of the Creative Commons Attribution 3.0 licence. Any further distribution of this work must maintain attribution to the author(s) and the title of the work, journal citation and DOI.

© 2014 IOP Publishing Ltd and Deutsche Physikalische Gesellschaft

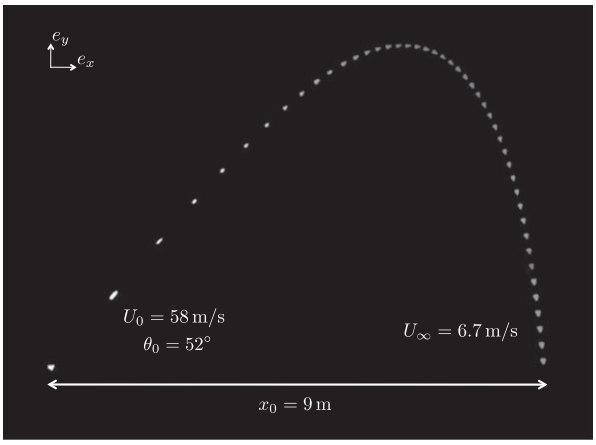

Figure 1. Chronophotography of a shuttlecock trajectory viewed from the side. The snapshots are separated by 50 ms. The shuttlecock, sent at 58 m s^{-1}, first decelerates, and it reaches its minimum velocity at the top of the trajectory, after which it re-accelerates in the gravity field and eventually falls almost vertically at constant speed.

One example of a ballistic trajectory is shown in figure 1 with a chronophotograph of a high clear in badminton. The shuttlecock, launched at $U_0 = 58$ m s^{-1} and $\theta_0 = 52°$, first goes straight, rapidly decelerates, then curves downwards, before falling nearly vertically at constant speed $U_\infty = 6.7$ m s^{-1}. It is striking how the projectile trajectory differs from a Galilean parabola: the trajectory does not present any left–right symmetry, and its range (defined as $x_0 \approx 9$ m in figure 1) is much shorter than expected for a parabolic behavior (240 m, for this angle and this velocity). This reduced range and the asymmetric shape both arise from the influence of air drag, which is now discussed.

Projectile trajectories are predicted by Newton's law, where we take into account both weight and air resistance, a quantity quadratic in velocity at large Reynolds numbers[3] [11]. In the absence of lift [12–14], it can be written as $M\mathrm{d}\mathbf{U}/\mathrm{d}t = M\mathbf{g} - \frac{1}{2}\rho S C_D U\mathbf{U}$, where $\mathbf{U}$ is the velocity of the projectile (and U its modulus), ρ the air density, $S = \pi R^2$ the cross-sectional area of the projectile, M its mass and C_D its drag coefficient[4]. This equation has a stationary solution ($M\mathrm{d}\mathbf{U}/\mathrm{d}t = \mathbf{0}$), for which drag balances weight. In this stationary limit, the velocity is aligned with gravity ($\mathbf{U} = -U_\infty \mathbf{e}_y$) with an intensity $U_\infty = (2Mg/\rho S C_D)^{1/2}$. This terminal velocity has been measured in a vertical wind tunnel and it is displayed in table 1 for different sports.

Comparing the initial velocity U_0 of the projectile to its terminal one U_∞ defines two regimes. For $U_0 < U_\infty$, air drag can be initially neglected and we expect the classical parabola, as observed in basketball. The opposite limit ($U_0 > U_\infty$) concerns most sports in table 1 if we take for U_0 the maximum recorded launching velocity $U_{\max} = \max(\mathrm{U}_0)$. The maximal ratio $U_{\max}/U_\infty \approx 20$ is achieved in badminton where the terminal velocity $U_\infty = 6.7$ m s^{-1} is much

[3] The Reynolds number compares the contributions of viscosity and inertia in the fluid motion. For an object of size $2R$ moving with the velocity U_∞ in a fluid of kinematic viscosity ν, it is written as $Re = 2RU_\infty/\nu$.

[4] The whole discussion is conducted assuming that C_D is constant for a given sport. This assumption is discussed in appendix B where the role of the drag crisis is considered.

Table 1. Characteristics of various sports projectiles: the diameter $2R$, mass M, and length of the field L_{field} are extracted from the official rules of the different federations. The sources for the maximum recorded speed $U_{\max}$ are: badminton [17, 18], tennis [19], table tennis [20], squash [21], jai alai [22], golf [23], volleyball [24], soccer [25], softball [26–28], baseball [29, 30], lacrosse [25], handball [31], and basketball [32]. The terminal velocities, U_∞, have been measured in a vertical wind tunnel [33]. The Reynolds number Re is calculated with the air viscosity $\nu = 1.5 \times 10^{-5}\,\mathrm{m^2\,s^{-1}}$. The drag coefficient C_D is linked to the mass and terminal velocity via the relation $C_D = 2Mg/(\rho U_\infty^2 \pi R^2)$. The aerodynamic distance $\mathcal{L}$ is U_∞^2/g. The last two columns present the calculated optimal angle $\theta_{\max}$ (equation (3)) and the corresponding maximal range $x_{\max}$ (equation (2)).

Sport	$2R$ (cm)	M (g)	L_{field} (m)	$U_{\max}$ (m s^{-1})	U_∞ (m s^{-1})	$Re = 2RU_\infty/\nu$	C_D	$(U_{\max}/U_\infty)$	$\mathcal{L}$ (m)	$\theta_{\max}$ (°)	$x_{\max}$ (m)
Badminton	6.0	5	13.4	137	6.7	3e + 04	0.64	20.4	4.6	22.1	14
Tennis	6.5	55	24	73	22	1e + 05	0.56	3.32	49.3	31.3	67
Table tennis	4.0	2.5	2.70	32	10	3e + 04	0.36	3.20	9.2	31.5	12
Squash	4.0	24	9.75	78	34	9e + 04	0.30	2.31	106	34.0	113
Jai alai	6.5	120	54.0	83	41	2e + 05	0.38	2.01	159	35.1	152
Golf	4.2	45	225	91	48	1e + 05	0.23	1.90	235	35.6	214
Volleyball	21	210	18	37	20	3e + 05	0.25	1.85	40.4	35.8	36
Soccer	21	450	100	51	30	4e + 05	0.24	1.70	90.2	36.5	75
Softball	9.7	190	76	47	33	2e + 05	0.38	1.42	113	37.9	80
Baseball	7.0	145	110	54	40	2e + 05	0.38	1.35	165	38.3	111
Lacrosse	6.3	143	100	50	48	2e + 05	0.35	1.04	215	40.1	110
Handball	19	450	40	27	36	5e + 05	0.20	0.75	132	41.9	45
Basketball	24	650	28	16	31	5e + 05	0.24	0.52	99.8	43.3	20

lower than the maximal recorded initial velocity $U_{\max} = 137\ \mathrm{m\ s^{-1}}$ [15–17]. A shuttlecock experiences no Magnus lift force since the only possible spin direction is aligned with the velocity, and its trajectory is strongly asymmetric, as seen in figure 1. We call this roughly triangular shape a Tartaglia curve in honor of Niccolo Tartaglia who first observed them in the context of cannonball paths [9]. In this limit ($U_0 > U_\infty$), the projectile weight can initially be neglected, so the equation of motion reduces to $dU/ds = -U/\mathcal{L}$, where $\mathcal{L} = 2M/\rho S C_D = U_\infty^2/g$ has the dimension of a length. Hence we expect a straight and exponentially decelerated path along the curvilinear coordinate s ($U(s) = U_0 e^{-s/\mathcal{L}}$). Slowing down takes place on this aerodynamic length $\mathcal{L}$, which only depends on the fluid and ball characteristics, scaling for example as $\rho_b R/\rho$ for a spherical ball of radius R and density ρ_b. (See appendix A for more details.)

However, the range of the projectile does not simply scale as $\mathcal{L}\cos\theta_0$, where θ_0 is the initial direction defined from the horizontal (figure 1). As the motion proceeds, the vertical component of the drag ($1/2\rho S C_D U U_y$) decreases, and it becomes equal to the weight Mg for $s = \mathcal{L}\ln(U_0/U_\infty(\sin\theta_0)^{1/2})$. Further, the projectile is mainly subjected to the action of gravity, which makes it fall nearly vertically (the gravitational part of the Tartaglia curve observed in figure 1). The corresponding range x_0, defined as the position on the horizontal axis where the projectile returns to its initial height, scales as $\mathcal{L}\cos\theta_0 \ln\left(U_0(\sin\theta_0)^{1/2}/U_\infty\right)$. On the one hand, contrasting with the case for parabolas, the range of a Tartaglia curve only weakly (logarithmically) depends on the initial velocity U_0: if you hit a ball harder, it will not go much further, a familiar feeling when you play badminton or strike a balloon. On the other hand, the range x_0 is expected to be a strong function of the angle θ_0, and is found from the latter expression to be maximum for an angle θ^* given at the leading order by $\tan\theta^* \approx 1/(2\ln(U_0/U_\infty))^{1/2}$. This angle deviates from the 45° value expected for a parabola, and it is all the smaller since the launch speed is high.

A more detailed calculation is presented in appendix A, and it extends previous theoretical discussions and numerical solutions [5, 6, 34, 35]. It yields an approximate analytical expression for the projectile range:

$$x_0 = \frac{1}{2}\mathcal{L}\cos\theta_0 \ln\left[1 + 4\left(\frac{U_0}{U_\infty}\right)^2 \sin\theta_0\right]. \tag{1}$$

At small velocity ($U_0 < U_\infty$), this expression reduces to the classical parabolic range, $x_0 = U_0^2 \sin(2\theta_0)/g$. For the opposite limit ($U_0 > U_\infty$), we recover both the scaling law derived above for x_0 and the angle θ^* maximizing this range. The optimal angle $\theta_{\max} = \theta^\star(U_{\max})$ and the maximum range $x_{\max} = x_0(U_{\max}, \theta_{\max})$ can be calculated as

$$x_{\max} = \frac{1}{2}\mathcal{L}\cos\theta_{\max} \ln\left[1 + 4\left(\frac{U_{\max}}{U_\infty}\right)^2 \sin\theta_{\max}\right], \tag{2}$$

with

$$\theta_{\max} = \arctan \sqrt{\frac{\left(U_{\max}/U_\infty\right)^2}{\left[1 + \left(U_{\max}/U_\infty\right)^2\right] \ln\left[1 + \left(U_{\max}/U_\infty\right)^2\right]}}\,. \tag{3}$$

In order to predict the maximal range for a given sport, one thus needs to know the distance $\mathcal{L} = 2\,M/\rho S C_D$ and the velocity ratio $U_{\max}/U_\infty$. These data are reported in table 1 for thirteen different sports. The ball properties (size $2R$ and mass M) and the size of the field (L_{field}) are prescribed by the different federations. They are respectively listed in columns 2, 3 and 4. The fastest hit velocity, $U_{\max}$, is obtained from the Guinness Book of Records or other sources detailed in the caption. The terminal velocity (U_∞) has been measured in a vertical wind tunnel for most of the sports [33]. The Reynolds number $Re = 2RU_\infty/\nu$, whose calculated value is given in column 7, ranges from 3×10^4 to 5×10^5. This large value justifies the expression for the drag used in the equation of motion. The drag coefficient is deduced from U_∞ and M. The velocity ratio $U_{\max}/U_\infty$ is presented in column 9 and is used to sort the different sports. Its value decreases from 20.4 for badminton to 0.52 for basketball. Most of the sports present a value larger than unity, which underlines the importance of aerodynamics in all these sports. Finally, calculated values of $\mathcal{L}$, $\theta_{\max}$ and $x_{\max}$ are given in the last three columns. It is found that $\theta_{\max}$ can strongly deviate from 45° (it is for instance 22.1° for badminton), and that $x_{\max}$ naturally varies to a large extent, from approximately 10 m for badminton or table tennis to 200 m for golf.

One way to understand the link between the range of the ball and the size of a sport field is to take the example of two players playing with a soft balloon. The common experience is that whatever the strength of the hit, the range of the balloon never exceeds $x_{\max} = 3$ m. Now imagine that the pitch is 100 m long with a net at the center: we expect the players to stay close to the net in a region of the order of the range. We thus anticipate the useful pitch distance to be comparable to the range. More generally, it is natural to compare the maximum projectile range deduced from equations (2) and (3) with the corresponding field length. This is done in figure 2 where we plot for each sport the size of the field, L_{field}, as a function of the associated ball's maximal range, $x_{\max}$. The equality $L_{field} = x_{\max}$ is underlined with a solid black line. It is remarkable that, without any free parameter for calculating $x_{\max}$, we observe a strong correlation between the maximal range and the field dimensions. This correlation implies that once a ball is chosen, one is able to calculate U_∞ and, knowing $U_{\max}$ (from the way of launching), it is then possible via equations (2) and (3) to predict the size of the field on which this game should be played.

Despite the strong correlation between L_{field} and $x_{\max}$, we also observe in figure 2 some deviations, to which we dedicate the last part of our study. We first start from the two strongest deviations stressed by red full squares. These points are associated with squash and jai alai. Since the field is much smaller than the range, these two sports are played with walls on the side to keep the ball in the field. They are the only 'immured' sports in our list. All the others are played on an open field. Apart from effecting a change in direction, the walls are used to decrease the time between two hits and these two sports are known to be characterized by strong accelerations and fast reflexes.

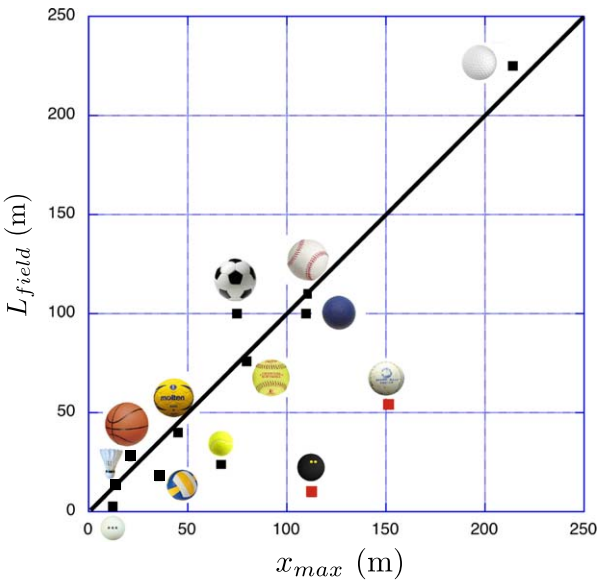

Figure 2. Correlation between the size of the sports field L_{field} for the different sports and the associated ball's maximum range, $x_{\max}$. The data are extracted from table 1. The solid line represents the equality between those two distances.

To complete our discussion about the length, we introduce the characteristic time $\tau_{sport} = L_{field}/U_{\max}$, that is, the time needed for the ball to move over the whole field length at the maximal speed. If τ_{sport} is shorter than the reaction time of a player, the sport involves reflexes and quick decisions. The reaction time τ of the player is the typical time needed to move over his/her own size. According to Keller [36, 37], this reaction time is of the order of one second ($\tau = 1$ s). The ratio $\tau_{sport}/\tau = L_{field}/(U_{\max} \,.\, \tau)$ is shown in figure 3 as a function of the distance ratio $L_{field}/x_{\max}$ for all the games of table 1.

In this graph, we identify two main families, the one in the bottom left corner and the one in the upper right corner. The first family includes squash, table tennis, tennis, volley and jai alai. It is characterized by a small field (compared to the range) and a small time (compared to the reaction time). The skills involved for this first family are thus reflexes and precision. In addition, for open fields (table tennis, tennis and volley), the property $L_{field} < x_{\max}$ implies that it is difficult to keep the ball within the limits. This difficulty is recognized by counting points whenever the ball goes out of the limits. In these games, players use topspin in order to reduce the ball range via the Magnus effect. Since one shot is enough to reach the opposite field, an obstacle is inserted to prevent, or to delay, an immediate scoring: for all these sports, a net is placed on the projectile path. Besides this, the inequality $\tau > \tau_{sport}$ implies that a player at rest will miss the ball if it is too far from him/her. This static situation is encountered during the serve and we observe that aces or winning serves are indeed possible.

The second main family of sports in figure 3 is composed of handball, baseball, softball, lacrosse, golf, soccer and basketball. The field is larger than the range, so it is not difficult to keep the ball within the limits. For the largest values of $L_{field}/x_{\max}$ (soccer and basketball), several shots are needed to move from one side to the other, which imposes passes and a collective game. Moreover the time of the sport is larger than the reaction time, so the player has

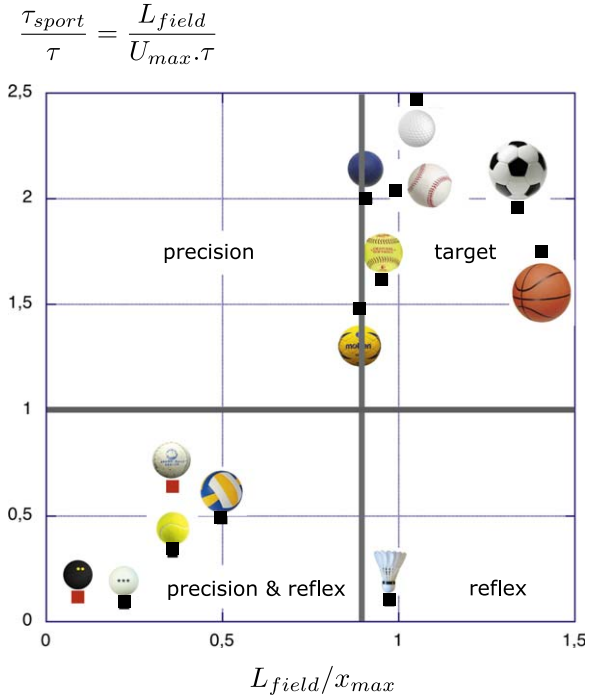

Figure 3. Classification of the different sports according to the distance ratio $L_{field}/x_{\max}$ and the time ratio $\tau_{sport}/\tau = L_{field}/U_{\max} \cdot \tau$.

enough time to reach the ball. As a common denominator, all the sports of the second family involve a target. The challenge is not the reflexes but the strategy and skill used in reaching this target (a goal for soccer and handball, a hole for golf, a basket for basketball).

Apart from these two main families, we find badminton in the bottom right corner of figure 3. This location underlines that the difficulty of the game is not staying within the limits of the field, but reacting within a very short time. For this reason, badminton can be defined as a pure reflex game. Finally, the upper left corner is empty here. For those games with a limited field (compared to $x_{\max}$) yet a large time (compared to τ), 'precision' is the main goal and we expect to find activities such as billiard, which are beyond the scope of the present study.

Sports fields have obviously been defined empirically, but their size, L_{field}, seems to be mainly fixed by the maximal range of the balls used to play, $x_{\max}$. We show this correlation in the first part of this study. In the second part, we define a phase diagram composed of two axes, one with the length ratio $L_{field}/x_{\max}$ and the other with the time ratio $L_{field}/U_{\max} \cdot \tau$ comparing the characteristic time of the game to the reaction time of the player. This diagram enables us to identify two main families, 'precision & reflex' sports and 'target' sports. This could be completed with 'precision' sports that have not been considered. Here, we have mainly considered sports where aerodynamic drag dominates. There are sports where lift plays a dominant role, such as Ultimate or even rugby and American football. A similar study for these lift sports remains to be done. Sports often are seen as metaphors of human activity, so our classification might more generally also reflect two main ways of acting, for example in science: intuition (with its shortcuts), as opposed to deduction (with its step-by-step approach). In this context, we find it symptomatic that Genia Peierls shared researchers between tennis players,

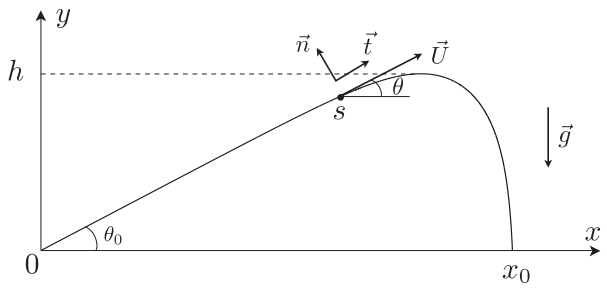

Figure 4. Parameters of the system.

who run toward the net to smash the ball and take advantage of the confrontation with an opponent, and golfers, who patiently push the ball many times until they reach the target [38]—that is, two sports opposed in our classification; de Gennes liked and used the Peierls analogy, and often stressed that we need both styles!

Acknowledgments

J W M Bush and D Legendre are gratefully acknowledged for valuable discussions and comments.

Appendix A

This appendix focuses on the main mathematical steps which lead to equation (1). It is extracted from a recent publication by the authors in the Proceedings of the Royal Society of London, Series A [33].

The projectile trajectory (figure 4) is predicted by Newton's law taking into account both the weight and the air resistance, which is quadratic in velocity at large Reynolds numbers. With the curvilinear location s, this equation is written as

$$MU\frac{d\mathbf{U}}{ds} = M\mathbf{g} - \frac{1}{2}\rho S C_D U \mathbf{U}, \tag{4}$$

where $\mathbf{U}$ is the velocity of the projectile (and $U = |\mathbf{U}|$), ρ the air density, $S = \pi R^2$ the cross-sectional area of the projectile, M its mass and C_D its drag coefficient. The projection of this equation on the x-axis leads to the horizontal velocity U_x:

$$U_x = U\cos\theta = U_0\cos\theta_0 \exp\left(-\frac{s}{2\mathcal{L}}\right), \tag{5}$$

where U_0 and θ_0 are respectively the initial velocity and the initial angle. $\mathcal{L} = M/\rho S C_D$ is the characteristic length of deceleration of the ball along the x-axis. We now project equation (4) along the direction $\vec{n}$:

$$U^2\frac{d\theta}{ds} = -g\cos\theta. \tag{6}$$

Using equation (5), we get a differential equation for θ. With the initial condition $\theta(s=0) = \theta_0$, this leads to

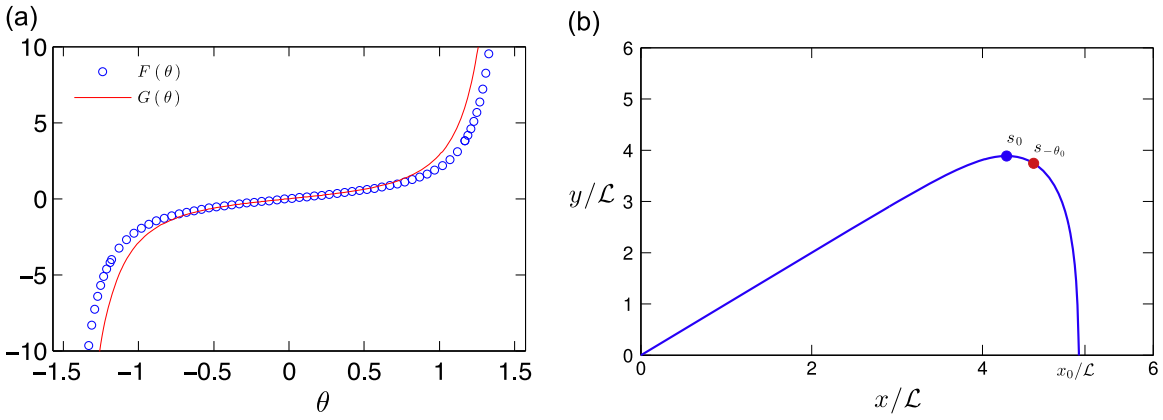

Figure 5. (a) Function F and its approximation G. (0b) Definition of $s_{-\theta_0}$.

$$\left[\ln\left(\frac{1+\sin u}{\cos u}\right)+\frac{\sin u}{\cos^2 u}\right]_{\theta}^{\theta_0}=\left(\frac{U_\infty}{U_0\cos\theta_0}\right)^2\left(e^{s/\mathcal{L}}-1\right) \tag{7}$$

Here, $U_\infty=\sqrt{2\,g\mathcal{L}}$ is the terminal velocity, i.e. the velocity that the ball gets when the drag compensates gravity. The function $F(u)=\ln\left(\frac{1+\sin u}{\cos u}\right)+\frac{\sin u}{\cos^2 u}$ can be approximated by $G(u)=2\sin u/\cos^2 u$ (figure 5(a)). To find the range x_0 of the trajectory, we make the approximation $x_0=s_{-\theta_0}\cos\theta_0$. $s_{-\theta_0}$ is the curvilinear location of the projectile for $\theta=-\theta_0$ (figure 5(b)).

With those approximations and equation (7), we find equation (1) of the paper:

$$x_0=\mathcal{L}\cos\theta_0\ln\left[1+4\left(\frac{U_0}{U_\infty}\right)^2\sin\theta_0\right]. \tag{8}$$

We now want to find the angle θ^* for which the range is maximal. We derive the expression for the range: $(dx_0/d\theta_0)_{\theta^*}=0$. This leads to $\tan\theta^*=\sqrt{X/(1+X)\ln(1+X)}$ with $X=4(U_0/U_\infty)^2\sin\theta^*$. This implicit equation is difficult to solve. We make the approximation $X\approx(U_0/U_\infty)^2$. The optimal angle becomes

$$\theta^\star=\arctan\sqrt{\frac{\left(U_0/U_\infty\right)^2}{\left[1+\left(U_0/U_\infty\right)^2\right]\ln\left[1+\left(U_0/U_\infty\right)^2\right]}}. \tag{9}$$

Equations (8) and (9) are discussed and tested numerically in a separate work [33].

Appendix B

The whole discussion on the size of the pitch has been conducted so far assuming a constant drag coefficient C_D. One could however be concerned by the fact that the ball may cross the drag crisis during its flight, which would change the drag coefficient and thus the trajectory. We discuss this effect in the present appendix.

Table 2. Columns 2 and 3 give the properties of the sports (initial velocity and launching angle) used to integrate the 'maximal' trajectory (figure 6(a)). The last two columns present the Reynolds number at which the drag crisis is expected, Re_c, and the corresponding jump in drag coefficient, $\Delta C_D/C_D = (C_{D+} - C_{D-})/C_{D-}$.

Sport	$U_{\max}$ (m s^{-1})	$\theta_{\max}$	C_D	Re_c	$\Delta C_D/C_D$
Badminton	137	22.1	0.64	n.o.	0
Tennis	73.0	31.3	0.56	n.o.	0
Table tennis	32.0	31.5	0.36	4e + 05	0.6
Squash	78.0	34	0.30	4e + 05	0.6
Jai alai	83.0	35.1	0.38	1.3e + 05	0.24
Golf	91.0	35.6	0.23	4e + 04	0.5
Volleyball	37.0	35.8	0.25	1.7e + 05	0.68
Soccer	51.0	36.5	0.24	1.5e + 05	0.58
Softball	47.0	37.9	0.38	1.3e + 05	0.24
Baseball	54.0	38.3	0.38	1.3e + 05	0.24
Lacrosse	50.0	40.1	0.35	4e + 05	0.6
Handball	27.0	41.9	0.20	1.5e + 05	0.58
Basketball	16.0	43.3	0.24	1.5e + 05	0.58

For each sport in table 1, we report in table 2 the Reynolds number Re_c at which the drag crisis occurs together with the jump in drag coefficient $\Delta C_D = (C_{D+} - C_{D-})/C_{D-}$. In this expression, C_{D+} and C_{D-} respectively stand for the drag coefficient after the crisis and that before the crisis. For golf, volley and baseball the values have been extracted from the work of Mehta [39]. For soccer, we have used data from [40]. For table tennis, squash, and lacrosse, we take the values corresponding to a smooth sphere [41]. For badminton [42] and tennis [43], no crisis has been observed. Due to ball similarity (and the lack of available data on the crisis), we assume that softball and jai alai have the same characteristics as baseball. Similarly the values for handball and basketball are supposed to be the same as for soccer.

Using these data, we computed the 'maximal' trajectory, using the fastest velocity $U_{\max}$ and the optimal angle $\theta_{\max}$ as initial conditions ($s = 0$), and integrated up to $s_{\max}$ where the particle returns to the ground ($y(s_{\max}) = 0$). For each sport concerned by the crisis, we report in figure 6(a) the evolution of the reduced Reynolds number, Re/Re_c, as a function of the normalized particle location, $s/s_{\max}$. The crisis is underlined by the horizontal thick line $Re/Re_c = 1$. The first striking observation is that very few sports cross the crisis during their 'maximal' trajectory. Some stay below (table tennis, squash, lacrosse) and most stay above (golf, soccer, handball, volleyball, jai alai, basketball). This first observation justifies the assumption of a constant drag coefficient.

However, we notice in figure 6(a) that two sports cross the line, namely baseball and softball. Focusing on baseball, we compare in figure 6(b) the trajectory obtained with a constant drag coefficient and the one obtained with a variable drag coefficient accounting for the crisis crossing. Since the drag coefficient increases as the ball moves from the supercritical to the subcritical region, we observe that the 'variable' trajectory leads to a smaller range. However, the ranges predicted by both calculations only differ by 7%. This difference is weak because the drag crisis occurs close to the maximum of the trajectory, after which the fall is close to vertical.

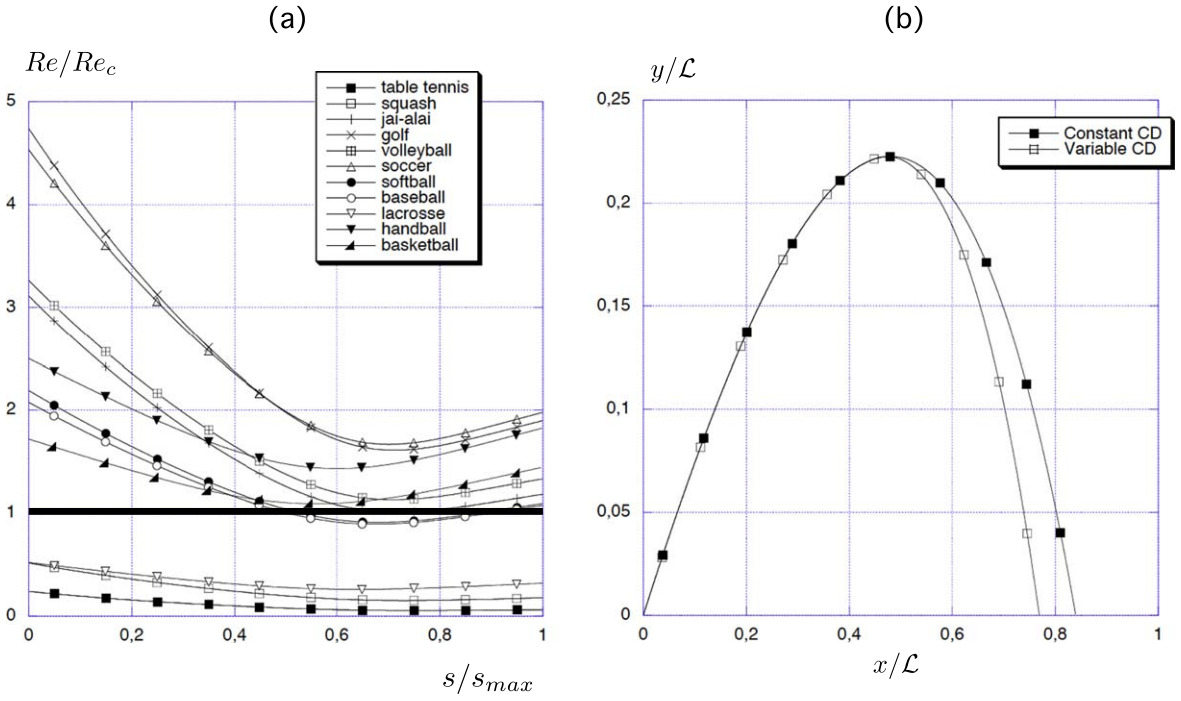

Figure 6. (a) Evolution of the reduced Reynolds number Re/Re_c along the 'maximal' trajectory, for the different sports presented in table 2 and affected by the crisis. The 'maximal' trajectory is defined by the trajectory obtained using as initial conditions the maximal velocity of the sport $U_{\max}$ and the optimal angle $\theta_{\max}$. (b) Comparison between the trajectory of a baseball ball calculated with a constant drag coefficient (■) and with a variable drag accounting for the crossing of the crisis (□).

Hence, even in this unfavorable case, the change in C_D only marginally affects our conclusions obtained with a constant drag assumption.

References

[1] Puhalla J, Krans J and Goatle M 1999 *Sports Fields: A Manual for Design, Construction and Maintenance* (Hoboken, NJ: Wiley)
[2] Charbonnier P 1904 *Traité de Balistique Extérieure* (Paris: Librairie Polytechnique)
[3] Metha D 1985 Aerodynamics of sports balls *Ann. Rev. Fluid Mech.* **17** 151–89
[4] Euler L 1755 Recherches sur la veritable courbe que decrivent les corps jettes dans l'air ou dans un autre fluide quelconque *Mem. Acad. Sci. Berl.* **9** 321–52
[5] de Mestre N 1990 *The Mathematics of Projectiles in Sport* (Cambridge: Cambridge University Press)
[6] Lamb H 1914 *Dynamics* (Cambridge: Cambridge University Press)
[7] Chudinov P S 2001 The motion of a point mass in a medium with a square law of drag *J. Appl. Math. Mech.* **65** 421–6
[8] Galilei G 1638 *Dialogues Concerning Two New Sciences* (Dover)
[9] Tartaglia N 1537 *Nova Scienta* (Venice)
[10] Tartaglia N 1846 *La Balistique* (Paris: Correard)
[11] Benjamin T B 1993 Note on formulas for the drag of a sphere *J. Fluid Mech.* **246** 335–42

[12] Magnus G 1853 Ueber die abweichung der geschosse, und eke auffallende erscheinung bei rotirenden korpern *Pogg. Ann. Phys. Chem.* **88** 1
[13] Barkla H M and Auchterloniet L J 1971 The magnus or robins effect on rotating spheres *J. Fluid Mech.* **47** 437–47
[14] Dupeux G, Le Goff A, Quéré D and Clanet C 2010 The spinning ball spiral *New J. Phys.* **12** 093004
[15] Cooke A J 2002 Computer simulation of shuttlecock trajectories *Sport Eng.* **5** 93–105
[16] Chen L-M, Pan Y H and Chen Y J 2009 A study of shuttlecock's trajectory in badminton *J. Sports Sci. Med.* **8** 657–62
[17] RIANOVOSTI sport article 2013 *Malaysian badminton star breaks smash speed record* (http://en.ria.ru/sports/20130823/182930446.html)
[18] Wikipedia contributors 2013 *Tan boon heong* (http://en.wikipedia.org/wiki/Tan_Boon_Heong)
[19] Wikipedia contributors 2013 *Fastest recorded tennis serves* (http://en.wikipedia.org/wiki/Fastest_recorded_tennis_serves)
[20] Jay Turberville 2003 *Table tennis ball speed* (www.jayandwanda.com/tt/speed.html)
[21] Wikipedia contributors 2013 *Cameron pilley* (http://en.wikipedia.org/wiki/Cameron_Pilley)
[22] Wikipedia contributors 2013 *Jai alai* (http://en.wikipedia.org/wiki/Jai_alai)
[23] Wikipedia contributors 2013 *Golf ball* (http://en.wikipedia.org/wiki/Golf_ball)
[24] Volleywood 2012 (www.volleywood.net/volleyball-related-news/volleyball-news-north-america/kaziyski-santos-lightning-spikes/)
[25] Guinness book of records 2013 (www.guinnessworldrecords.com/news/2013/7/how-the-serves-at-wimbledon-compare-to-the-speed-of-other-sports-by-infographic-49476/)
[26] Russell D A 2008 *Explaining the 98-mph bbs standard for asa softball* (www.acs.psu.edu/drussell/bats/bbs-asa.html)
[27] Alam F, Ho H, Smith L, Subic A, Chowdhury H and Kumar A 2012 A study of baseball and softball aerodynamics *Procedia Engineering* **34** 86–91
[28] Nathan A M 2003 Characterizing the performance of baseball bats *Am. J. Phys.* **71** 134–43
[29] eFastball 2009 *Batted ball speed* (www.efastball.com/hitting/average-bat-speed-exit-speed-by-age-group/%url)
[30] Greenwald R M, Penna L H and Crisco J J 2001 Differences in batted ball speed with wood and aluminum baseball bats: a batting cage study *J. Appl. Biomech.* **17** 241–52
[31] Gorostiaga E M, Granados C, Ibanez J and Izquierdo M 2005 Differences in physical fitness and throwing velocity amongelite and amateur male handball players *Int. J. Sports Med.* **26** 225–32
[32] Huston R L and Cesar A G 2003 Basketball shooting strategies—the free throw, direct shot and layup *Sports Eng.* **6** 49–64
[33] Cohen C, Darbois-Texier B, Dupeux G, Brunel E, Quéré D and Clanet C 2014 The aerodynamical wall *Proc. R. Soc. Lond.* A **470** 20130497
[34] Erlichson H 1983 Maximum projectile range with drag and lift with particular application to golf *Am. J. Phys.* **51** 357–62
[35] Chudinov P S 2010 Approximate formula for the vertical asymptote of projectile motion in midair *Int. J. Math. Educ. Sci. Technol.* **41** 92–8
[36] Keller J B 1973 A theory of competitive running *Phys. Today* **26** 43–5
[37] Keller J B 1974 Optimal velocity in a race *Am. Math. Mon.* **81** 474–80
[38] Peierls R E 2007 *Sir Rudolf Peierls: Selected Private and Scientific Correspondence* (Singapore: World Scientific)
[39] Mehta R D 2008 Sports ball aerodynamics ed H Norstrud *Sport Aerodynamics* (New York: Springer)
[40] Asai T, Seo K, Kobayashi O and Sakashita R 2007 Fundamental aerodynamics of the soccer ball *Sports Eng.* **10** 101–10
[41] Mehta R D and Pallis J M 2001 Sports ball aerodynamics: Effects of velocity spin and surface roughness ed S Froes and S J Haake *Mater. Sci. Sports* 185–97

[42] Cooke A J 1999 Shuttlecock aerodynamics *Sports Eng.* **2** 85–96
[43] Mehta R D, Alam F and Subic A 2008 Aerodynamics of tennis balls—a review *Sports Technol.* **1** 1–10